Talanta 83 (2010) 162–166

Contents lists available at ScienceDirect

Talanta

journal homepage: www.elsevier.com/locate/talanta

Direct electrochemistry of hemoglobin immobilized in CuO nanowire bundles

Yueming Li[a,1], Qian Zhang[b,1], Jinghong Li[a,*]

[a] Department of Chemistry, Key Laboratory of Bioorganic Phosphorus Chemistry and Chemical Biology, Tsinghua University, Beijing 100084, China
[b] College of Chemistry, Liaoning University, Shenyang 110036, China

ARTICLE INFO

Article history:
Received 11 June 2010
Received in revised form 28 August 2010
Accepted 30 August 2010
Available online 8 September 2010

Keywords:
Copper Oxide
Nano-structured materials
Bioelectrochemistry
Biosensor

ABSTRACT

It is one of main challenges to find the suitable materials to enhance the direct electron transfer between the electrode and redox protein for direct electrochemistry field. Nano-structured metal oxides have attracted considerable interest because of unique properties, well biocompatibility, and good stability. In this paper, the copper oxide nanowire bundles (CuO NWBs) were prepared via a template route, and the bioelectrochemical performances of hemoglobin (Hb) on the CuO NWBs modified glass carbon electrodes (denoted as Hb-CuO NWBs/GC) were studied. TEM and XRD were used to characterize the morphology and structure of the as synthesized CuO NWBs. Fourier transform-infrared spectroscopy (FT-IR) proved that Hb in the CuO NWBs matrix could retain its native secondary structure. A pair of well-defined and quasi-reversible redox peaks at approximately −0.325 V (vs. Ag/AgCl saturated KCl) were shown in the cyclic voltammogram curve for the Hb-CuO NWBs/GC electrode, which indicated the direct electrochemical behavior. The Hb-CuO NWBs/GC electrode also displayed a good electrocatalytic activity toward the reduction of hydrogen peroxide. These results indicate that the CuO NWBs are good substrates for immobilization of biomolecules and might be promising in the fields of (bio) electrochemical analysis.

1. Introduction

The research of direct electrochemistry for redox proteins is very important, which not only helps to elucidate the intrinsic thermodynamic and kinetic properties of proteins but also fabricate bioelectronic devices [1,2]. The direct electron transfer between redox protein and electrode can particularly offer a route for mediator-free and sensitive biosensors, thus can simplify the detection system for less reagent and better stability [3]. Unfortunately, the direct electrochemistry for most redox proteins on conventional electrodes is a great challenge due to the deeply buried redox-active center in the proteins and unfavorable orientations of protein molecular on electrode surface [3,4]. Therefore, one of main challenges in this field is to get the suitable materials to enhance the direct electron transfer between the electrode and redox protein.

In recent years, nano-structured metal oxides especially one dimensional (1D) nanomaterial have been paid considerable attention due to their unique optical, electrical, and magnetic properties [5,6] and also have attracted considerable interest in the bioanalytical area because of their large specific surface area, high aspect ratio, well biocompatibility, easy preparation and good stability [7,8]. The ordered nanowire arrangements such as nanowire arrays or nanowire bundles can possess more advantages over single nanowire in electrochemical filed [9]. On one hand, the nanowires have direct 1D electronic pathways allowing for efficient charge transport. On the other hand, the space between neighboring nanowires can facilitate the diffusion of electrolyte which is important for electrochemistry and may also provide suitable sites for fixing bio-molecular used in direct electrochemistry.

Copper oxide (CuO) has been extensively studied with respect to its applications such as heterogeneous catalysts [10,11], gas sensors [12], electrochemical materials [13–15], field emission emitter [16,17], paramagnetic material [18] and high Tc superconductor [19]. The CuO nanowire has recently been introduced into the field of bioelectrochemistry with a promising future because of plentiful properties as well as low price and no toxicity [20]. Thus it will be very interesting to investigate the typical bioelectrochemical behaviors of redox proteins immobilized in the CuO nanowires bundles.

In this paper, we report the preparation of CuO nanowire bundles (CuO NWBs) via a hard-template route. The direct electrochemical behaviors of hemoglobin (Hb) on the CuO NWBs based glassy carbon (GC) electrode (denoted as Hb-CuO NWBs/GC electrode) were investigated. Moreover, the electrocatalysis of the modified electrodes toward hydrogen peroxide was also studied. A quasi-reversible electrochemistry behavior of immobilized Hb was obtained on the Hb-CuO NWBs/GC electrode. Furthermore, such

* Corresponding author. Tel.: +86 10 62795290.
E-mail address: jhli@mail.tsinghua.edu.cn (J. Li).
[1] Both the authors contributed equally to this paper.

0039-9140/$ – see front matter © 2010 Elsevier B.V. All rights reserved.
doi:10.1016/j.talanta.2010.08.056

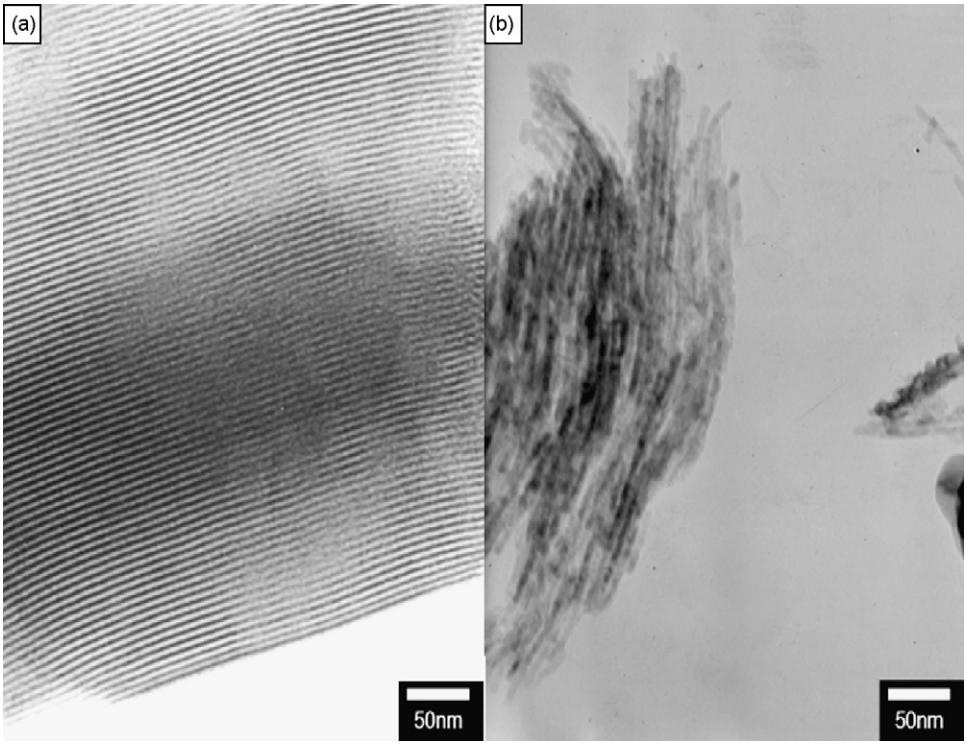

Fig. 1. TEM images of SBA-15 (a) and CuO nanowire bundles (NWBs) (b).

modified electrode displayed a fast heterogeneous electron transfer rate, fairly good sensitivity, wide linear range and excellent stability to the detection of hydrogen peroxide.

2. Materials and methods

2.1. Materials

Hemoglobin (Hb, MW 66,000) was supplied by Sigma Chemical Co. Copper dichloride ($CuCl_2{\cdot}2H_2O$), oxalic acid, sodium hydroxide (NaOH), hydrogen peroxide (H_2O_2, 30%) and hydrochloric acid (HCl, 37%) were purchased from Beijing Chemical Plant. Polyvinyl alcohol (PVA, MW. 14,000), tetraethyl orthosilicate and P123 ($EO_{20}PO_{70}EO_{20}$, MW 5800) were purchased form Aldrich. All reagents were of analytical-grade reagents and used without further purification. Double distilled de-ionized water was used for making all the solutions.

2.2. Preparation of CuO nanowire bundles

The calcinated mesoporous SBA-15 (1D pore structure) which served as the hard-template was prepared by adding tetraethyl orthosilicate (TEOS) into the hydrochloric acid solution of triblock copolymer P123 according to previous report [21]. To prepare copper oxide nanowire bundles, 1 g of SBA-15 was dispersed in 10 ml of 4 M $CuCl_2$ aqueous solution, then the composites were treated by vacuum filtration. A certain amount of saturated oxalic acid was added to the composites during vacuum filtration. The composites were dried at 60 °C in oven until a constant weight. Subsequently, the resultant composites were heated at 500 °C for 2 h in air, forming black powders. Finally, the obtained black powders were soaked in 2 M NaOH solution for 20 h to remove the hard-template, then thoroughly washed with distilled water and dried at 60 °C in oven.

2.3. Preparation of CuO NWBs/GC, Hb/GC and Hb-CuO NWBs/GC electrodes

Prior to use, GC electrodes with a diameter of 3 mm were polished on a polishing cloth with 1.0, 0.3, 0.05 μm alumina powder in sequence, rinsed with de-ionized water, and sonicated in acetone, ethanol and de-ionized water, respectively. Then, the electrodes were blow-dried under a nitrogen stream at room temperature. The CuO NWBs modified electrodes were prepared by a simple casting method. Typically, a homogeneous solution (Solution I, pH 7.0) containing 1.5 mg ml^{-1} PVA, 2 mg ml^{-1} CuO NWBs and 4 mg ml^{-1} Hb was prepared by adding certain volume of PVA solution, CuO NWBs suspension and Hb solution (dissolved in 50 mM pH 7.0 phosphate-buffered solution (PBS)) into 50 mM pH 7.0 PBS buffer. Solution I (7 μl) was then cast onto the surface of a freshly polished GC electrode by using a syringe to prepare the Hb-CuO NWBs/GC electrode. To get a uniform film on the surface of the electrodes, water was slowly evaporated in a beaker with a cover. The dried Hb-CuO NWBs/GC electrode was stored at 4 °C in refrigerator when not in use. Solution II (containing 1.5 mg ml^{-1} PVA, 4 mg ml^{-1} Hb) was used in this experiment for comparison. And CuO NWBs/GC electrode was prepared with the same procedures as described using solution II.

2.4. Characterization

The morphologies of the samples were observed by a JEOL-1010 Transmission Electron Microscopy (TEM). The wide angle powder X-ray diffraction (XRD) measurement was performed on Bruker D8-Advance X-ray powder diffractometer with Cu Kα radiation (λ = 1.5406 Å) using a graphite monochromator, while the low-angle XRD was carried out in Rigaku D/max-RB X-ray powder diffractometer with Cu Kα radiation (λ = 1.5406 Å) using a graphite monochromator. The data were collected at the range between 10° and 80° (2θ) at the scanning rate of 8°/min for wide angle XRD

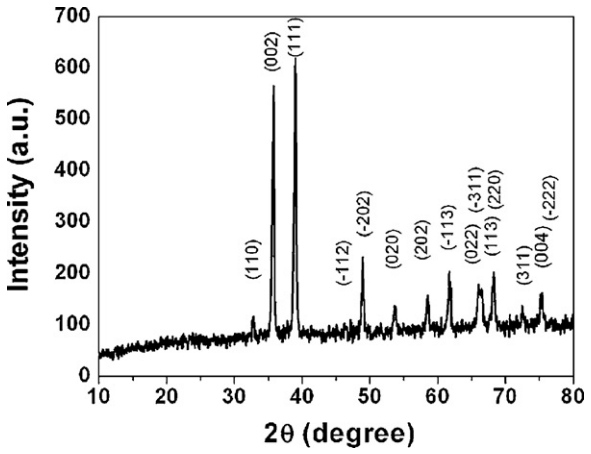

Fig. 2. Small angle XRD pattern and wide angle XRD pattern (inset) of CuO NWBs.

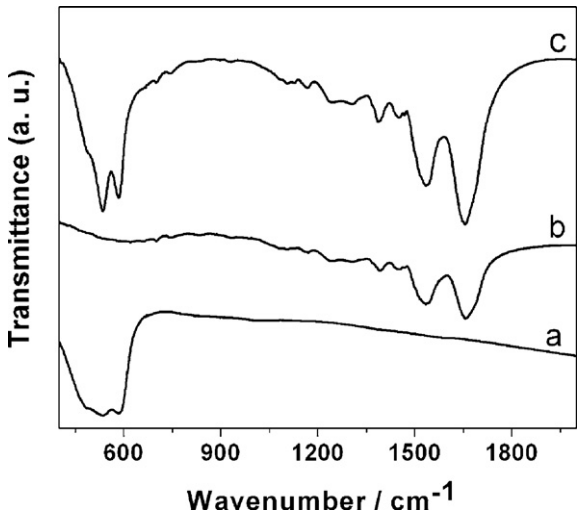

Fig. 3. FT-IR spectra of CuO nanowire (a), Hb (b) and Hb-CuO NWBs composites (c).

and 0.7° and 10° (2θ) at the scanning rate of 1°/min for low-angle XRD, respectively. Fourier transform-IR (FT-IR) spectra were carried out through a Perkin-Elmer spectrophotometer operating in the infrared domain between 400 and 2000 cm^{-1} by a KBr matrix.

Electrochemical measurements were performed at room temperature using a CHI 830 workstation (CH Instruments, Inc., Austin, USA). The measurements were based on a three-electrode system with the as-modified protein electrode as the working electrode, the platinum foil as the counter electrode, and a saturated Ag/AgCl electrode as the reference electrode. Without additional statement, 0.1 M pH 7.0 PBS was used as the electrolyte in all experiments. The buffer solution was purged with highly purified nitrogen for at least 30 min and all the electrochemical measurements were carried out under nitrogen atmosphere environment.

3. Results and discussion

Morphologies of as-prepared SBA-15 and CuO NWBs were observed via TEM. As shown in Fig. 1a, the high quality SBA-15 template which possesses the typical characteristic of 1D nanochannel about 6–9 nm in diameter is presented, which is favoring to prepare 1D nano-structures [22,23]. In the preparation process, copper oxalate formed precipitates in the 1D channel of template first due to its small solution product constant ($K_{sp} = 4.43 \times 10^{-10}$). During calcination under air atmosphere, the copper oxalate precipitates were oxidized to copper oxide. At the same time, the 1D channel of template limited the diameter of CuO, leading the formation of CuO nanowire bundles. As seen from Fig. 1b, the as-prepared copper oxide exhibited morphologies of nanowire bundles, which is like the replica of SBA-15. Each single nanowire has a diameter of about 5–8 nm and a length of several hundred nanometers.

The wide angle XRD was used to determine the crystal phase of as-prepared samples. As shown in the inset of Fig. 2, the crystalline phase of the CuO NWBs belongs to monoclinic phase space group Cc (no. 9), which is in good agreement with copper oxide (JCPDS-ICDD 80-1916). As evidenced by the TEM, the spacing between CuO nanowire bundles belongs to the mesoporous scope. However, there were no characteristic peaks of mesoporous materials in the low-angle region in the small angle XRD pattern, indicating disordered mesoporous structure of nanowire bundles [24].

FT-IR is an efficient tool to probe the secondary structure for immobilized proteins and the perturbation of protein can be observed from the changes of the spectrum. The FT-IR spectra of Hb, Hb-CuO NWBs and CuO NWBs are shown in Fig. 3. The high-frequency mode at about 585 cm^{-1} is reported to be a Cu–O stretch along the [$\bar{2}$02] direction, and the mode at about 535 cm^{-1} is related to Cu–O stretch along [202] [25,26]. Fig. 3b shows the IR spectrum of Hb, which exhibits adsorption bands at 1657 and 1534 cm^{-1}, attributing to the shapes of the amides I and II infrared absorbance bands of Hb respectively. These peaks can provide the detail information on the secondary structure of the polypeptide chain. The amide I band (1700–1600 cm^{-1}) is caused by C=O stretching vibrations of peptide linkages in the protein backbone. The amide II band (1620–1500 cm^{-1}) results from a combination of N–H bending and C–N stretching [27]. As shown in Fig. 3c, the amide I and II bands of Hb/CuO NWBs (1655 and 1535 cm^{-1}) are nearly the same as those obtained for native Hb, and the characteristic bands of CuO NWBs are close to those of original CuO NWBs. These results suggest that Hb immobilized with CuO NWBs retains its native structure.

The typical cyclic voltammograms (CVs) for the Hb-CuO NWBs/GC electrode and CuO NWBs/GC electrode in 0.1 M PBS (pH 7.0) over the potential range from 0.2 to −0.7 V at scan rate of 200 mV s^{-1} are shown in Fig. 4. No obvious redox peak is observed at the CuO NWBs/GC electrode, suggesting that the CuO NWBs is not electroactive in the potential range defined. Because the redox center heme FeIII/FeII is deeply seated in a large protein shell, it is difficult for Hb to obtain direct electrochemical transfer on the bare GC electrode independently. Therefore, the cyclic voltammograms of the Hb/GC electrode in PBS did not show any response under the same conditions. However, a pair of stable and well-defined quasi-reversible redox peaks is observed at the Hb-

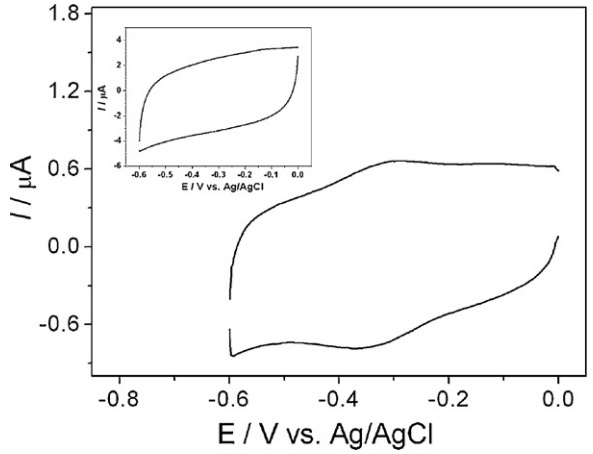

Fig. 4. Cyclic voltammograms of Hb-CuO NWBs/GC and CuO NWBs/GC (Inset) electrodes in 0.1 M PBS (pH 7.0). Scan rate, 200 mV s^{-1}.

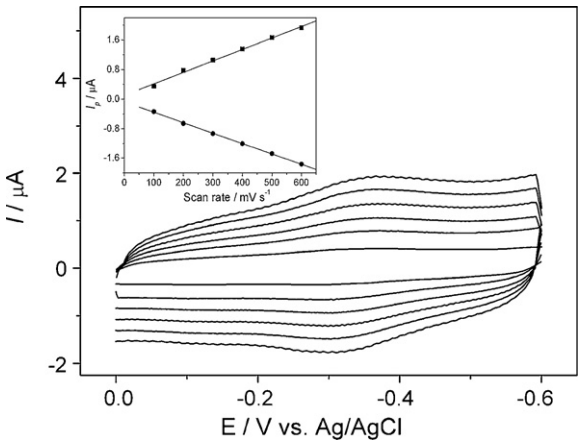

Fig. 5. Cyclic voltammograms of Hb-CuO NWBs/GC electrode at scan rate of 100, 200, 300, 400, 500 and 600 mV s^{-1} in 0.1 M PBS (pH 7.0), respectively. Plots of oxidation peak current and reduction peak current vs. scan rate for Hb-CuO NWBs/GC electrode (inset).

CuO NWBs/GC electrode, which could be ascribed to the direct electron transfer between the Hb and the underlying electrode. The cathodic and anodic peak potentials are −0.30 and −0.35 V, respectively and the formal potential is −0.325 V, which is consistent with literatures [28]. This pair of peaks are attributed to the reversible redox processes of heme group in immobilized Hb proteins: Hb–Fe(III) ↔ Hb–Fe(II) [29]. The separation of cathodic and anodic peak potentials was 50 mV and the ratio of oxidation and reduction peak currents was approximately 1 at the scan rate of 200 mV s^{-1}, demonstrating that all electroactive ferrous Hb (Hb–Fe(II)), which was produced by reduction of ferric Hb (Hb–Fe(III)) on the forward scan, can be oxidized to Hb–Fe(III) on the reverse scan. By comparison, it is obviously that CuO NWBs play an important role in this system in that they may not only be capable of anchoring the Hb, but also a matrix to provide a friendly and conductive microenvironment for the anchored Hb to achieve direct electron transfer.

The effect of scan rates on the response of the Hb-CuO NWBs/GC electrode is shown in Fig. 5. Both the reduction and oxidation currents (I_p) increase linearly with increasing of the scan rates (inset), suggesting that the redox processes of the immobilized Hb in the CuO NWBs based film belong to a surface-confined process. The linear regression equations are: $y = 0.104 + 0.00309x$, $r = 0.9973$ (anodic peak), and $y = -0.0698 - 0.00283x$, $r = 0.9997$ (cathodic peak). According to Faraday's law, $Q = nFA\Gamma^*$ (where F is the Faraday constant and Γ^* represents the surface concentration of electroactive Hb, Q can be calculated by integrating the reduction peak of Hb, n stands for the number of electrons transferred, and A represents the area of the electrode surface, here using the geometric area of the GC electrode (0.07 cm^2)), the surface concentration of electroactive Hb (Γ^*) at the Hb-CuO NWBs/GC electrode is calculated to be 5.86×10^{-10} mol cm^{-2}, which is higher than the theoretical monolayer value (1.89×10^{-11} mol cm^{-2}) [30]. The result indicates that several layers of Hb entrapped in the CuO NWBs based film participate in the electron transfer process. It could be speculated that the biocompability of the Hb-CuO NWB/GC electrode should be attributed to the multi-layer electron transfer process.

The detection of hydrogen peroxide (H_2O_2) is very important in the field of environment, industry, chemistry, food, pharmacy and biology [31]. The typical methods to determinate H_2O_2 include titrimetry, spectrometer, chemluminescence and electrochemical methods. Among these methods, the electrochemical technique based on direct electrochemistry for determination of H_2O_2 possesses the advantages of intrinsic selectivity and sensitivity of

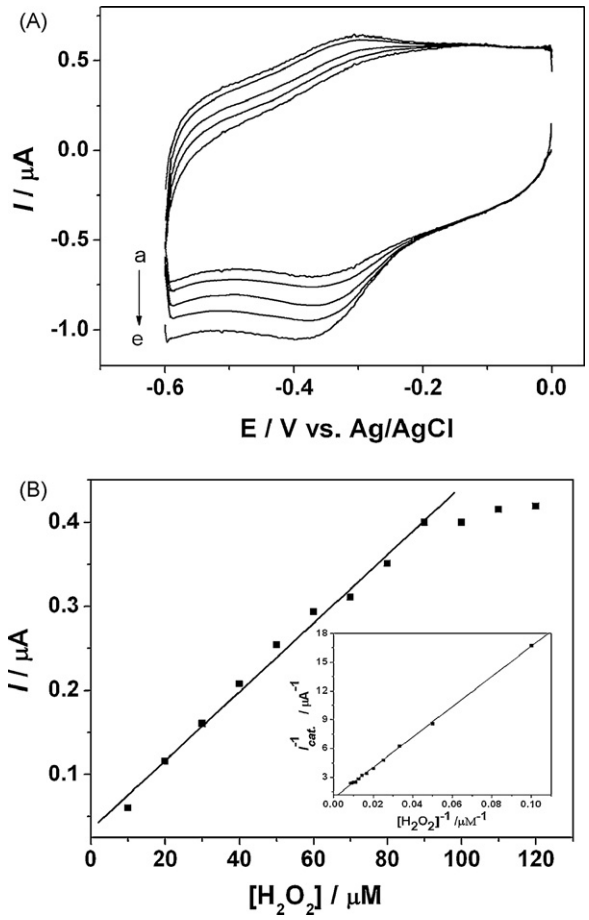

Fig. 6. (A) Cyclic voltammograms of the Hb-CuO NWBs/GC electrode in 0.1 M PBS (pH 7.0) solution with (a) 0, (b) 10, (c) 30, (d) 50, and (e) 90 μM H_2O_2. Scan rate, 200 mV s^{-1}. (B) Plot of the electrocatalytic current (Icat) vs. H_2O_2 concentration for the Hb-CuO NWBs/GC electrode in 0.1 M PBS solution (pH 7.0) and the relative Lineweaver–Burk plot (inset).

enzymatic reactions, which is promising for fabricating simple and low-cost enzyme sensors [32]. As a very important protein with ability of oxygen binding, Hb has close structural similarity to the peroxidase with an intrinsic catalytic activity toward peroxide compounds [33]. To check the bioelectrocatalytic activity of the Hb-CuO NWBs/GC electrode to the reduction of H_2O_2, cyclic voltammetric experiments were performed. As shown in Fig. 6a, when H_2O_2 was added to a pH 7.0 PBS solution, an obvious increase of the reduction peak current at about −0.35 V was observed, accompanied by the decrease of the oxidation peak current. However, no peak was observed in the CVs of Hb/GC electrode in the presence of H_2O_2 in the potential range of −0.6–0 V. Therefore, the above results prove that Hb immobilized in the CuO NWBs based film keeps its original bioelectrocatalytic activity. The mechanisms can be expressed as the following:

$$\text{Hb[Heme(FeIII)]} + H_2O_2 \rightarrow \text{Compound1} + H_2O \quad (1)$$

$$\text{Compound1} + H_2O_2 \rightarrow \text{Hb[Heme(FeIII)]} + H_2O + O_2 \quad (2)$$

$$\text{Hb[Heme(FeIII)]} + H^+ + e^- \rightarrow \text{Hb[Heme(FeII)]atelectrode} \quad (3)$$

$$\text{Hb[Heme(FeII)]} + O_2 \rightarrow \text{Hb[Heme(FeII)]} - O_2\text{fast} \quad (4)$$

$$\text{Hb[Heme(FeII)]} - O_2 + H^+ + e^- \rightarrow \text{Hb[Heme(FeII)]} + H_2O_2\text{atelectrode} \quad (5)$$

The cathodic peak currents increase linearly with the concentration ranges of H_2O_2 from 10 to 90 μM, shown in Fig. 6b. The linear regression equation is $y = 0.00409x + 0.0348$ ($R = 0.995$, $n = 9$), where y and x stand for the peak current (μA) and the concentration (μM) of H_2O_2, respectively. The sensitivity of the Hb-CuO NWB/GC is 0.0576 A cm^{-2} M^{-1} and the detection limit of the protein electrode is 3.3 μM when the signal to noise ratio is 3. Based on the Lineweaver–Burk equation, the apparent Michaelis–Menton constant (K_M) could be calculated [34]. In this experiment, the Lineweaver–Burk plot shows a K_M of 176.33 μM for Hb-CuO NWB/GC electrode (Fig. 6b, inset), which is lower than other Hb modified electrode [35,36]. The small K_M shows a good affinity between the immobilized Hb and H_2O_2, favoring electrochemical reaction.

The CuO NWBs modified electrodes have improved the catalytic reduction of H_2O_2, and this might be contributed to the properties of copper oxide and the unique structures of nanowires bundles. The bundles are composited of nanowires whose pores belong to mesoporous scope, thus they possess the advantages of 1D materials as well as mesoporous materials. On one hand, the 1D nano-structure helps to achieve efficient charge transport. On the other hand, the pores between neighboring nanowires play an important role, which provide suitable sites to fix biomolecular. Since the pores between the bundles are not uniform, the large pores can provide sufficient space to immobilize large size Hb proteins and give the immobilized Hb a suitable microenvironment to keep their bioactivities. At the same time, the small pores between bundles help to alleviate the mass-transport resistance by providing "substrate-transport channels" and enhance the catalytic performance for electrode consequently [37]. Compared with previously reported metal oxide modified electrode, the surface concentration of electroactive Hb (Γ^*) of Hb-CuO NWB/GC electrode was higher than that of the Hb-Nafion-Co_3O_4/GC electrode [7,38], the linear response range and the Michaelis–Menton constant (K_M) were better that those of the Hb/ZrO_2/DMSO/PG electrode. However, the limited detection and sensitivity were not good as reported electrodes [7].

To investigate the reproducibility of the Hb-CuO NWBs/GC electrode, six parallel experiments were done with GC electrodes and the results prove that there was an acceptable reproducibility with a relative standard deviation of 3.3% for the current determined at 30 μM H_2O_2. The long-term stability of the biosensor was evaluated over a 30-day period. The electrodes were stored in PBS (pH 7.0) at 4 °C when not in use. The current response to 30 μM H_2O_2 for Hb-CuO NWBs/GC electrode decreased only about 5% after a 30-day period, indicating the good long-term stability. These results show that the CuO NWBs based hybrid film was a suitable matrix to immobilize Hb with retaining its bioactivity.

4. Conclusions

We have demonstrated the preparation of CuO NWBs using SBA-15 as the template, and characterized them by XRD, TEM and FT-IR. The experiments to immobilize the Hb showed that the CuO NWBs would not destroy the structure of Hb, indicating the good biological compatibility. The electrochemical experiments proved that Hb-CuO NWBs/GC electrode not only shows a fast direct electron transfer of Hb but also displays good electrocatalytic response to H_2O_2. The good performance of Hb-CuO NWBs/GC electrode may be related to the unique nano-structures of CuO NWBs, which could provide a favorable microenvironment around Hb to retain its bioactivity and high loading. Therefore, CuO NWBs might provide a new promising platform for further study on the direct electrochemistry of other redox proteins and the development of new type of biosensors for real sample analysis.

Acknowledgements

This work was financially supported by the National Natural Science Foundation of China (No. 20975060 and 20901035) and National Basic Research Program of China (No. 2007CB310500).

References

[1] C. Legar, S.J. Elloitt, K.R. Hoke, L.J.C. Jeuken, A.K. Jones, F.A. Armstrong, Biochemistry 42 (2003) 8653.
[2] A. Heller, Acc. Chem. Res. 23 (1990) 128.
[3] X.J. Zhang, H.X. Ju, J. Wang, Electrochemical Sensors, Biosensors and Their Biomedical Applications, Elsevier, New York, 2008.
[4] A. Riklin, E. Katz, I. Williner, A. Stockerand, A.F. Buckmann, Nature 376 (1995) 672.
[5] F. Favier, E.C. Walter, M.P. Zach, T. Benter, R.M. Penner, Science 293 (2001) 2227.
[6] Y.N. Xia, P.D. Yang, Y.G. Sun, Y.Y. Wu, B. Mayers, B. Gates, Y.D. Yin, F. Kim, H.Q. Yan, Adv. Mater. 15 (2003) 353.
[7] X.B. Lu, G.F. Zou, J.H. Li, J. Mater. Chem. 17 (2007) 1427.
[8] S.J. Bao, C.M. Li, J.F. Zang, X.Q. Cui, Y. Qiao, J. Guo, Adv. Funct. Mater. 18 (2007) 591.
[9] Y.M. Li, X.J. Lv, J.H. Li, Appl. Phys. Lett. 95 (2009) 113102.
[10] J.B. Reitz, E.I. Solomon, J. Am. Chem. Soc. 120 (1998) 11467.
[11] J.A. Switzer, H.M. Kothari, P. Poizot, S. Nakanishi, E.W. Bohannan, Nature 425 (2003) 490.
[12] V. Chowdhuri, V. Gupta, K. Sreenivas, R. Kumar, S. Mozumdar, P.K. Patanjali, Appl. Phys. Lett. 84 (2004) 1180.
[13] P. Poizot, S. Laruelle, S. Grugeon, L. Dupont, J.M. Tarascon, Nature 407 (2000) 496.
[14] X.P. Gao, J.L. Bao, G.L. Pan, H.Y. Zhu, P.X. Huang, F. Wu, D.Y. Song, J. Phys. Chem. B 108 (2004) 5547.
[15] M.J. Song, S.W. Hwang, D.M. Whang, Talanta 80 (2010) 1648.
[16] T. Hsieh, J.M. Chen, H.H. Lin, H.C. Shih, Appl. Phys. Lett. 83 (2003) 3383.
[17] J. Chen, S. Deng, N. Xu, W. Zhang, X. Wen, S. Yang, Appl. Phys. Lett. 83 (2003) 746.
[18] M.O. Keefe, F.S. Stone, J. Phys. Chem. Solids 23 (1962) 161.
[19] J.G. Bendnorz, K.A.Z. Muller, Phys. B: Conens. Matter 64 (1986) 189.
[20] Z.J. Zhuang, X.D. Su, H.Y. Yuan, Q. Sun, D. Xiao, M.M.F. Choi, Analyst 133 (2008) 126.
[21] Y. Zhao, Q.S. Huo, J.L. Feng, B.F. Chmelka, G.D. Stucky, J. Am. Chem. Soc. 120 (1998) 6024.
[22] S.C. Laha, R. Ryoo, Chem. Commun. (2003) 2138.
[23] H. Kim, J. Cho, J. Mater. Chem. 18 (2008) 771.
[24] Q. Hu, Z.H. Gao, X.R. Yang, J. Sol–Gel Sci. Technol. 44 (2007) 171.
[25] T. Premkumar, K.E. Geckeler, Small 2 (2006) 616.
[26] G. Kliche, Z.V. Popovic, Phys. Rev. B 42 (1990) 10060.
[27] J.K. Kauppinen, D.J. Moffatt, H.H. Mantsch, D.G. Cameron, Appl. Spectrosc. 35 (1981) 71.
[28] Q. Zhang, L. Zhang, J.H. Li, J. Phys. Chem. C 111 (2007) 8655.
[29] N.Q. Jia, L.J. Wang, L. Liu, Q. Zhou, Z.Y. Jiang, Electrochem. Commun. 7 (2005) 349.
[30] Q. Zhang, L. Zhang, B. Liu, X.B. Lu, J.H. Li, Biosens. Bioelectron. 23 (2007) 695.
[31] X.B. Lu, Q. Zhang, L. Zhang, J.H. Li, Electrochem. Commun. 8 (2006) 874.
[32] S.S. Razola, B.L. Ruiz, N.M. Diez, H.B. Mark, J.M. Kauffmann, Biosens. Bioelectron. 17 (2002) 921.
[33] S.A. Adediran, A.M. Lambeir, Eur. J. Biochem. 186 (1989) 571.
[34] R.A. Kamin, G.S. Wilson, Anal. Chem. 52 (1980) 1198.
[35] C.X. Cai, J. Chen, Anal. Biochem. 325 (2004) 285.
[36] G. Zhao, J.J. Feng, J.J. Xu, H.Y. Chen, Electrochem. Commun. 7 (2005) 724.
[37] L. Zhang, Q. Zhang, J.H. Li, Electrochem. Commun. 9 (2007) 1530.
[38] S.Q. Liu, Z.H. Dai, H.Y. Chen, H.X. Ju, Biosens. Bioelectron. 19 (2004) 963.